ANALYSIS OF DAM RESPONSE FOR FOUNDATION FAULT RUPTURE

Lelio Mejia[1] and Ethan Dawson[2]

SUMMARY

Considerable knowledge and experience has been developed over the past 40 years in the engineering profession regarding the seismic performance and analysis of dams for earthquake shaking. However, comparatively limited experience is available regarding the evaluation of dams for the effects of foundation fault rupture during earthquakes. This paper examines the factors to be considered in the evaluation of embankment dams for foundation faulting, and illustrates the analysis of dam response under foundation faulting by means of a case history, the seismic evaluation of Aviemore Dam.

INTRODUCTION

Numerous observations of dam performance during earthquakes have been accumulated by the engineering profession over the past 40 years and constitute a valuable database of experience with the performance of dams subjected to earthquake shaking. Beginning with the seminal work of Newmark [1] and Seed [2], significant progress has also been made over the same period in developing procedures to evaluate the effects of earthquake shaking on dams. On the other hand, modest experience is available regarding the performance of dams under foundation fault rupture and few studies on the subject have been reported in the literature. Although insightful research into the response of embankment dams to foundation faulting has been carried out in recent years (e.g., [3], [4]), procedures for the analysis of foundation rupture effects on dams have not been well established.

The purpose of this paper is to present an overview of the factors to be considered in the evaluation of embankment dams for earthquake fault rupture in the foundation. The paper describes an approach to analyze the effects of foundation faulting on embankment dam stability and illustrates the analysis of dam deformations under foundation fault rupture through the case history of the seismic safety evaluation of Aviemore Dam. The dam forms part of the Aviemore Power Station, a hydroelectric facility located on the Waitaki River in the South Island of New Zealand. Although, the evaluation of dams for foundation faulting must consider the effects of simultaneous earthquake shaking, this paper deals primarily with the shearing effects of foundation rupture.

GENERAL CONSIDERATIONS

In addition to strong earthquake shaking, coseismic offset of the foundation of an embankment dam by fault surface displacement can be expected to result in shearing and distortion of the embankment. Previous research (e.g., [3], [4]) indicates that the degree of shearing and the extent to which the rupture will propagate upwards within the embankment will depend on the magnitude of the fault displacements and on the stiffness of the embankment materials.

Propagation of the rupture within a zoned embankment will result in offset of the impervious core, shells, filters and other zones that make up the embankment. The embankment deformations are also likely to result in cracking and consequent leakage. If shearing or cracking of the core or main water barrier occurs, a key concern will be the ability of the embankment and foundation to handle potential leakage without development of internal erosion or piping. This will depend on two main factors: a) the erodibility of the embankment and foundation materials, and b) the extent to which filter and drainage zones remain continuous and functional across the zone of shearing to prevent internal erosion and migration of materials and development of a piping or instability failure mechanism.

Thus, the key issues associated with shearing of an embankment dam by foundation fault rupture may generally be summarized as follows:

- The extent to which the rupture will propagate from the foundation upwards within the embankment.
- The amount of distortion and offset of the embankment and of the dam's main water barrier, for example an impervious core, which might lead to cracking and leakage.
- The location and extent of cracking, and the amount of leakage resulting from such cracking and general distortion of the embankment.
- The resistance of the embankment and the foundation materials to internal erosion under the flow velocities associated with increased seepage or exposure to direct leakage.
- The amount of offset and distortion of the embankment zones, such as filter and drainage zones, designed to control seepage and leakage.
- The ability of filter and drainage zones to remain functional after offset and distortion and prevent internal erosion from developing into continued erosion.
- The potential for piping through the embankment and/or foundation due to continued internal erosion of the embankment and foundation materials.

[1] *Principal Engineer, URS Corporation, Oakland, California, USA*

[2] *Senior Project Engineer, URS Corporation, Los Angeles, California, USA*

- The capacity of pervious downstream embankment zones to pass-through leakage flowing through piping or erosion channels, without slope or toe erosion and instability.

APPROACH TO EVALUATION OF FOUNDATION FAULT RUPTURE EFFECTS

The general approach to address the key issues associated with fault rupture of an embankment dam and analyse its performance under the effects of such rupture consists of the following steps.

1. Performing a numerical analysis to calculate the deformations and stresses induced in the dam by the foundation displacements associated with the fault rupture.
2. Evaluating the shear offset of the embankment zones, in particular of the core and filter and drainage zones, from the calculated deformations.
3. Based on the stresses calculated from the analysis, estimating the location and extent of cracking of the core and other embankment zones.
4. Estimating potential leakage through cracks in the core and assessing the erodibility of the core and other embankment materials.
5. Based on the calculated embankment deformations and stresses, evaluating the post-rupture continuity and functionality of filter and drainage zones.
6. Assessing the potential for continued erosion of the embankment and foundation materials considering the post-rupture functionality of filter and drainage zones.
7. Evaluating the through-flow resistance of any pervious downstream embankment zones.
8. Assessing the likelihood of piping failure based on the potential for continued erosion and development of piping channels within the embankment and foundation and on the through-flow resistance of the embankment.

Application of the above approach to the analysis of a large embankment for the effects of foundation fault displacement is illustrated by means of the case history of the seismic evaluation of Aviemore Dam.

AVIEMORE DAM

Aviemore Dam is a composite structure built in the 1960s, consisting of a 364 m long, 56 m high concrete gravity section, and a 430 m long, 49 m high earth embankment. It has an approximately 12 m wide crest, which supports a 7 m wide paved road. The dam retains a reservoir with a volume of 530×10^6 m^3 and a surface area of 28.8 km^2, with a minimum operating freeboard of 2.8 m. In view of the potential consequences of a dam failure, the dam is classified as a high hazard structure. An aerial view of the dam is shown in Figure 1.

The dam design was conceived to accommodate the variable geology and presence of the Waitangi Fault in the dam foundation. The fault crosses the embankment foundation about 30 m from the interface with the concrete dam, and strikes near normal to the dam axis. The concrete dam and the embankment left (east) of the fault are founded on greywacke of Mesozoic age. Right (west) of the fault, the earth dam is founded on Tertiary claystones and sandstones with interbedded coal seams and Quaternary alluvial and fan gravels.

As shown in Figure 2, the earth dam is a zoned embankment with an upstream sloping impervious core flanked by pervious shoulders. A sand filter separates the core from the downstream shoulder, and blankets the bottom of the core trench under the shoulder. The internal geometry varies along the length of the embankment because the core is flared as it approaches the concrete dam (Figure 2b). The core consists of medium plasticity silty clay. The filter is comprised of well-graded sand and is approximately 1 m thick. Broadly graded sandy gravels with cobbles and boulders make up the shoulders.

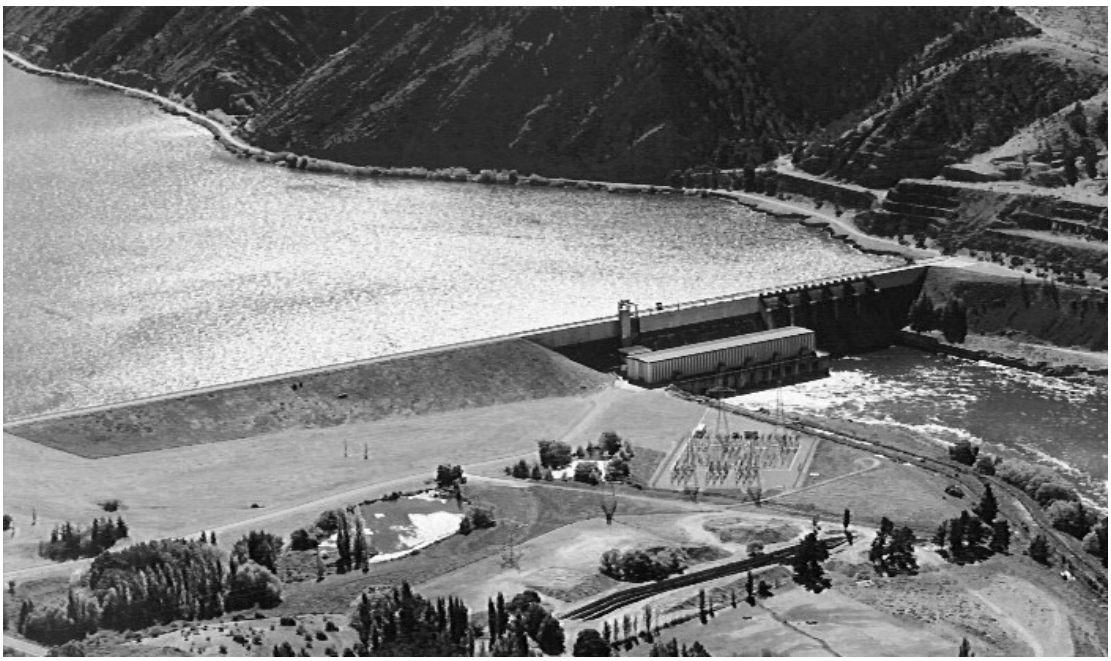

Figure 1. Aerial view of Aviemore Dam.

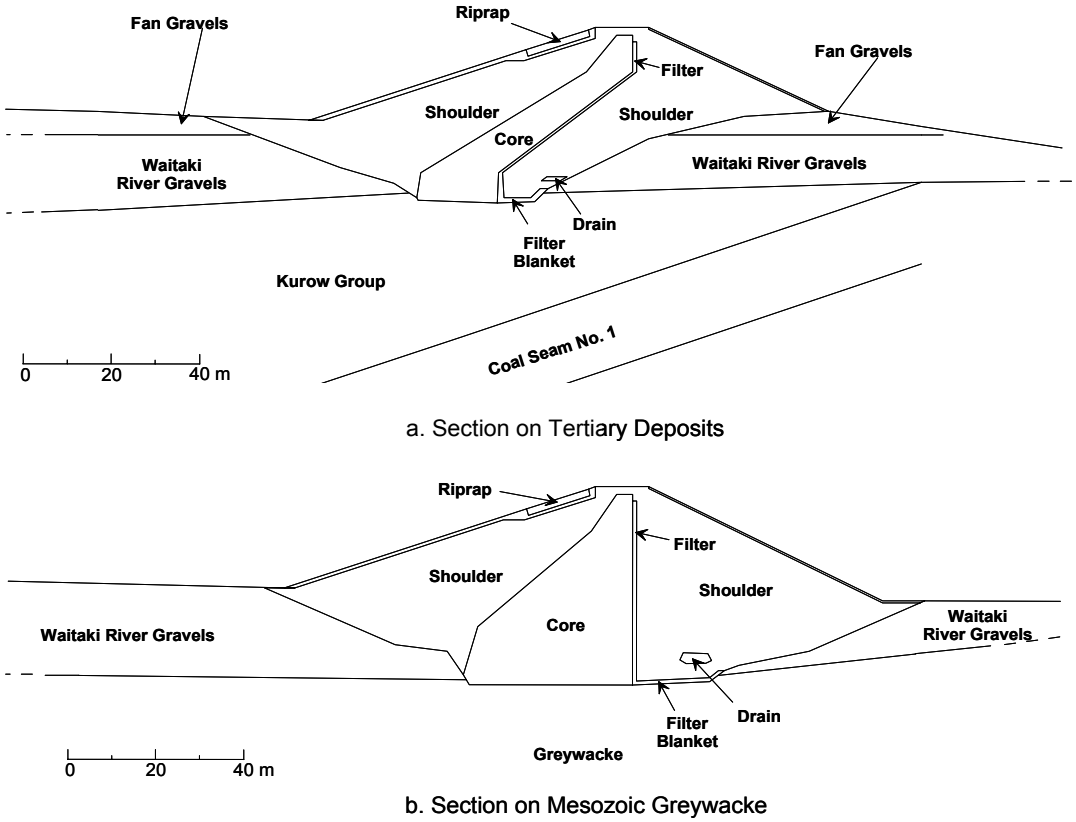

Figure 2. Representative Embankment Cross Sections.

SEISMIC EVALUATION CRITERIA

The dam is located in a region of sparse seismicity about 100 km east of the boundary between the Pacific and Australian plates. The seismotectonics of the region are controlled by the relative motion between the two plates, which results in slip along the Alpine Fault and continental collision and uplift of New Zealand's Southern Alps [5].

During construction of the dam, the Waitangi Fault was recognized in the foundation excavation but was not considered to be active. However, trenches excavated recently along the fault have disclosed late Quaternary single-event vertical displacements of 1 to 2 m, upwards on the embankment dam side. The most recent displacement on the fault in the dam area occurred 13,000 to 14,000 years ago, and at least two, and possibly three, movements have occurred in the last 21,000 ± 1,000 years [6].

The criteria used to define the Safety Evaluation Earthquake (SEE) for analysis of the dam has been described by Mejia et al. [7]. The maximum earthquake on the Waitangi fault, a magnitude M_w 7.0 event, was adopted as the SEE. The 84th percentile response spectrum was adopted to represent the SEE vibratory ground motion. The corresponding peak horizontal acceleration on hard rock is about 1.0 g. A fault vertical separation of 1.2 m and a horizontal to vertical displacement ratio (H:V) of 1:3 were adopted to define the SEE fault surface displacement at the site. Additional details of the characteristics of the SEE ground motions and fault displacements, and the procedures used to develop them, are presented by Mejia *et al.* [8]. The SEE characteristics included the reservoir floor displacements for analysis of reservoir dynamic response and dam overtopping potential.

GENERAL APPROACH TO SEISMIC EVALUATION

The seismic safety evaluation of the dam focused on those project facilities that, if seriously damaged during the SEE, could result in uncontrolled release of the reservoir. The key issues addressed in the dam's seismic safety evaluation included: its stability under strong earthquake shaking, its integrity under foundation fault rupture, the potential for reduction in reservoir storage and for seiche and consequent dam overtopping, and the seismic performance of the appurtenant works. Only the analyses of the embankment dam for foundation fault rupture will be discussed herein. Other aspects of the evaluation are discussed by Walker *et al.* [9] and Mejia *et al.* [10].

Evaluation of the dam's response to earthquake shaking required consideration of the dynamic response characteristics of the concrete section relative to those of the embankment dam, and of the interaction between the two dams. Although analytical tools are available to perform a three-dimensional (3-D) dynamic analysis of the entire structure, such type of analysis was deemed impractical. Instead, each dam was analyzed separately using two-dimensional (2-D) models that accounted for changes in geometry along the longitudinal axis and that properly represented material behaviour, foundation and reservoir interaction, and ground motion differences from one dam foundation to the other. The effects of interaction between the two dams were inferred from the calculated response of the 2-D models on both sides of the concrete-embankment interface.

Because the concrete dam is located on the downthrown block about 30 m away from the upthrown block, surface rupture of the Waitangi Fault is expected to shear the earth dam but not disrupt the concrete dam foundation significantly. Reverse faulting typically will not result in major disruption of the downthrown block. Furthermore, because the Mesozoic greywacke rock of the downthrown block is much stronger than the Tertiary deposits of the upthrown block, it is unlikely that significant shear deformations will extend into the downthrown block.

Shearing of the embankment by foundation fault rupture, will occur concurrently with the earthquake shaking. Although the effects of foundation rupture will be compounded with those

of shaking, the embankment shearing will be driven primarily by the foundation displacements. Thus, the dam response to foundation rupture was analyzed separately from its response to earthquake shaking.

ANALYSIS FOR FOUNDATION FAULT RUPTURE

Analysis Approach

Offset of the dam foundation by the SEE fault surface displacements is expected to result in shearing and distortion of the dam embankment. Propagation of the rupture within the embankment will result in offset of the filter and might juxtapose the core and downstream shoulder materials if the filter were to be sheared over its full thickness. The embankment deformations may also result in cracking and leakage.

The structural deformation response of the dam to the SEE fault surface displacement was analyzed using the 3-D finite difference program FLAC^{3D} [11]. The finite difference mesh shown in Figure 3 was developed based on the geometry of the embankment and alluvium at the location where the fault crosses the dam foundation. The base of the model was offset at this location to simulate the fault surface displacements. The mesh consists of approximately 40,000 elements and 40,000 nodes. All three components of displacement were imposed simultaneously: vertical separation, dip-slip, and strike-slip. These displacements were applied to the base and sides of the up-thrust portion of the model, while displacements were fixed for the base and side boundaries of the down-thrust portion.

Benchmark analyses were performed to compare the results obtained with FLAC^{3D} with previously published numerical results [3]. In addition, benchmark analyses of simplified 2-D models of the embankment materials were conducted to facilitate interpretation of the results obtained with the 3-D model.

Materials Stress-Strain Models

Two alternative constitutive models were used to represent the stress-strain properties of the dam and foundation materials because these properties are not known with certainty. The first model is based on the hyperbolic stress-strain model described by Duncan *et al.* [12]. The second model is derived from the small-strain dynamic shear modulus, G_{max}, together with the normalized modulus (G/G_{max}) reduction relationships for the materials, and is referred to as the G/G_{max}-based model. Those two models were assumed to bracket the stress-strain behaviour of the materials given that fault rupture loading is likely to induce large strains at relatively high strain rates. The model parameters were obtained from laboratory testing, field shear wave velocity measurements, and published data for similar materials.

Numerical and laboratory studies have shown that post-peak strain softening and dilation strongly affect the localization of strains and the propagation of fault rupture [4]. Therefore, those aspects of material behaviour were included in both stress-strain models.

The stress-strain relationships described by the hyperbolic model of Duncan et al. and by the G/G_{max} relationships can adequately represent the behaviour of the materials at stress levels below the peak strength. However, they are not capable of representing post-peak behaviour. Accordingly, the stress-strain models of the materials were composed of two parts. The first part corresponds to strains ranging from zero to the value at peak strength. The second part corresponds to strains ranging from the value at peak strength to large values in the steady state range. In the first part, the hyperbolic-based models were defined to match the hyperbolic model of Duncan et al. appropriate to each material. Likewise, the G/G_{max}-based models were defined to match the backbone curve corresponding to each material. In the second part, both stress-strain models were defined to produce strain softening and dilation appropriate to each type of material.

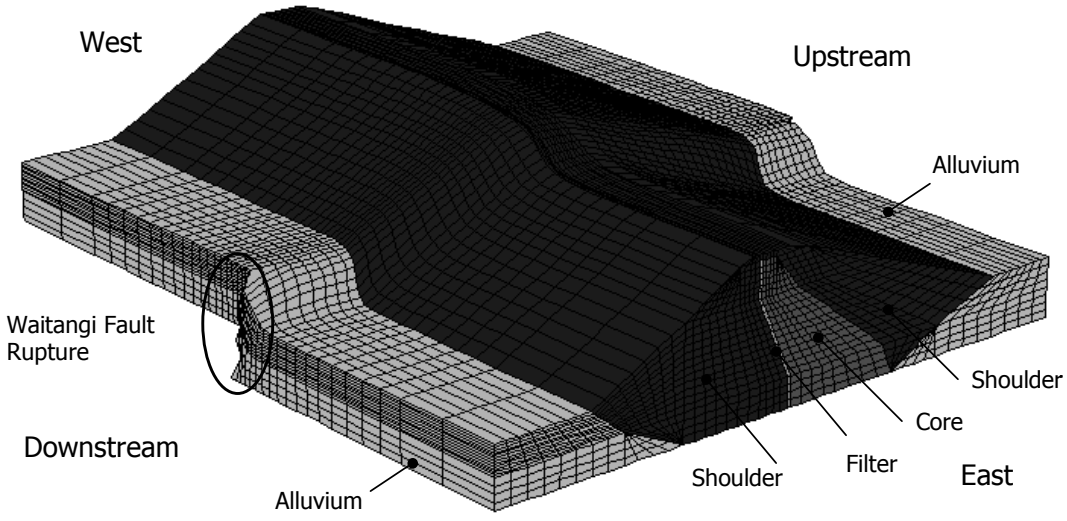

Figure 3. Three-dimensional Mesh of Dam for Analysis of Foundation Rupture.

The shoulder and alluvium gravels have index properties (e.g. gradations, particle shapes, specific gravities) and densities that are very similar to those of the Oroville Dam gravels. Thus, the parameters for the hyperbolic Duncan et al. model for the shoulder and alluvium gravels were obtained from the laboratory test data presented by Marachi [13] for the Oroville gravels. The parameters of the hyperbolic model for the core materials were obtained from the results of consolidated-undrained triaxial compression tests on undisturbed samples obtained from borings in the core. The hyperbolic model parameters for the embankment materials are listed in Table 1. Together with the formulation of the hyperbolic model of Duncan *et al*., those parameters define the first part of the hyperbolic-based stress-strain models for the embankment materials.

Table 1. Parameters of Duncan *et al.* [12] hyperbolic model used in analysis for embankment materials.

Parameter*	Shoulder and Alluvial Gravels	Core Material
Friction Angle at 1 atm Confining Pressure, φ_o	51º	0
Friction Angle Decrement, $\Delta\varphi$	6º	0
Undrained Strength or Cohesion, S_u (kPa)	0	$0.01\sigma'_m$ + 110**
Young's Modulus Number, K	1780	131
Young's Modulus Exponent, n	0.39	0.25
Failure Ratio, R_f	0.67	0.67
Bulk Modulus Number, K_b	1300	***
Bulk Modulus Exponent, m	0.16	***

*Refer to Duncan *et al.* [12] for definition of parameters.
**σ'_m is mean effective stress in kPa.
***Bulk modulus computed from Young's modulus assuming a Poisson's ratio of 0.49.

For the G/G_{max}-based model, the backbone curve for each material was obtained from the value of G_{max} and from the modulus reduction relationship appropriate to such material. The values of G_{max} were obtained from in-situ shear wave velocity measurements in the embankment and foundation. The modulus reduction relationships were selected based on the index characteristics of the materials and published information for similar materials. The values of G_{max} and the modulus relationships of the materials are tabulated in Table 2. The backbone curves calculated from those parameters, together with the bulk moduli listed in Table 2, defined the first part of the G/G_{max}-based models.

The amounts of strain-softening and dilation for the shoulder and alluvium gravel materials were modelled to match those observed in triaxial compression tests on Oroville gravels reported by Marachi [13]. In contrast, based on the results of the triaxial compression tests on the core materials, no strain softening is expected in those materials. Likewise, because the core materials are expected to behave in an undrained manner under fault rupture loading, dilation of those materials is not expected under such loading. Thus, no strain softening or dilation was included in the stress-strain models for the core materials.

The hyperbolic and G/G_{max}-based models were implemented using FLAC's built-in strain hardening-softening model. This is a Mohr-Coulomb plasticity formulation in which the friction angle, cohesion, and dilation angle can be specified as a function of plastic shear strain. Incrementally, the formulation follows elastic-perfectly plastic behaviour, but at each numerical integration step, the friction angle, cohesion, and dilation angle are updated by user-input functions of the computed plastic shear strain. For stress points inside of the yield surface, the model behaves as linear-elastic, and linear-elastic behaviour is assumed for unloading and reloading.

As an example, the stress-strain and volume change behaviour simulated by the hyperbolic-type model for the shoulder and alluvium gravels is illustrated in Figure 4, as a function of effective minor principal stress. It may be seen that the model stress-strain and volume change relationships incorporate the effects of strain softening and dilatancy and their dependency on effective confining pressure.

Table 2. Parameters of G/G_{max}-based model used in analysis for embankment materials.

Parameter*	Shoulder Gravels	Alluvial Gravels	Core Material
Maximum Shear Modulus, G_{max} (kPa)	$7.25(10)^4\ \sigma'^{½}_m$**	$7.25(10)^4\ \sigma'^{½}_m$	$600S_u$***
Modulus Reduction Relationship, G/G_{max}	Average for Sands by Seed and Idriss [14]	Average for Sands by Seed and Idriss [14]	Clays with Plasticity Index of 30 by Vucetic and Dobry [15]
Bulk Modulus, K (kPa)	$9.37(10)^4\ \sigma'^{½}_m$	$1.83(10)^5\ \sigma'^{½}_m$	****

*Refer to Seed and Idriss [14] for definition of parameters.
**σ'_m is mean effective stress in kPa.
***S_u is undrained shear strength in kPa from Table 1.
****Bulk modulus computed from maximum shear modulus, G_{max}, assuming a Poisson's ratio of 0.49.

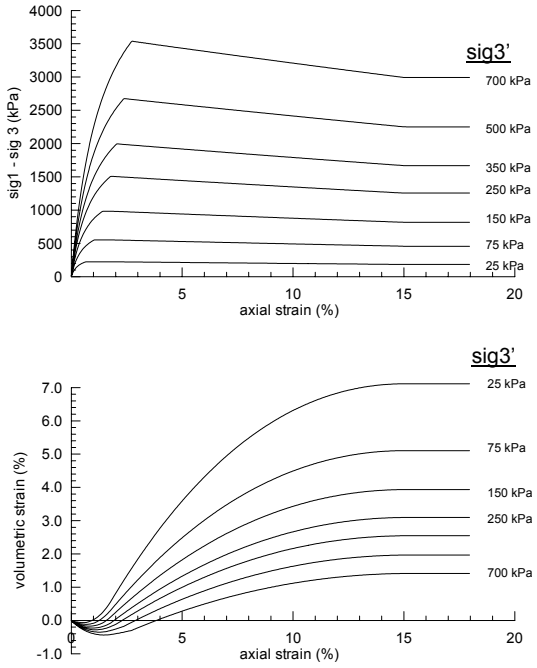

Figure 4. Stress-strain and Volume Change Behaviour of Hyperbolic Model for Shoulder and Alluvium Gravels.

ANALYSIS RESULTS

The 3-D finite difference mesh was used to calculate deformations and stresses throughout the embankment for various amounts of fault vertical separation (FVS). The calculated deformations were used to evaluate the nature and extent of embankment distortion, and the calculated stresses were used to infer the extent of propagation of the fault rupture within the embankment and to estimate the extent and depth of cracking.

The extent of rupture propagation within the embankment was inferred from the calculated contours of stress level (SL). This is defined as the ratio of the deviatoric stress to the strength of the material, as follows:

$$SL = \frac{(\sigma_1 - \sigma_3)}{(\sigma_1 - \sigma_3)_f} \quad (1)$$

where: σ_1 = Major principal stress;
σ_3 = Minor principal stress;
and *f* denotes the condition at failure.

Bray el al. [16] found that this is a convenient parameter to track the propagation of fault rupture through soil, and that the 95% stress level contour is a good indicator of the length of the rupture zone. This is because a stress level of 95% approximately marks the development of shear failure in the material.

An illustration of the stress levels calculated using the hyperbolic model is shown in Figure 5. This figure shows the stress level on a longitudinal section of the embankment cut 10 m downstream of the crest centreline and calculated for 0.5 m of FVS. Stress levels on this section are representative of stress levels in a large portion of the embankment. It may be seen that the model predicts propagation of the rupture to about one-half the height of the embankment, based on the 95% stress level criterion discussed above. The analyses for the full range of potential fault displacements indicate that the rupture should reach the crest surface at a FVS of 0.7 m. The analyses using the G/Gmax-based model indicate that the rupture should reach the crest at a FVS of 0.4 m.

The calculated distributions of stresses and displacements indicate that the zone of embankment deformation in response to the fault surface rupture will likely be several tens of meters long, extending from west of the vertical projection of the foundation fault offset (see Figure 5) to near the concrete dam. Shear offset of the filter for the SEE was calculated from the calculated rupture propagation within the embankment for a FVS of 1.2 m. Figure 6 shows the shear offsets of the filter calculated using the two constitutive models assumed for the dam materials. Those results indicate that the chimney filter is not expected to be fully offset anywhere along its height during the SEE. This is the case notwithstanding the fact that the filter has jagged edges, resulting from construction layering, as opposed to the smooth profile shown in Figure 6. However, full offset is expected to occur across the filter blanket extending downstream over the foundation because the blanket is about 0.9 m thick.

The extent and depth of cracking was assessed based on the calculated changes in the state of stress within the embankment due to fault rupture. Because the embankment materials, including the core material, are likely to have a low tensile strength, cracking may be assumed to develop when the effective minor principal stress, σ_3', drops to very low values or becomes tensile. A zero tensile strength was assumed for all embankment materials in the numerical analysis to simulate their low tensile strength.

Figure 7 shows the change in σ_3' along a longitudinal section cut through the crest centreline, for a FVS of 1.2 m. Such change is expressed as the difference between the final and initial values of σ_3' normalized by the initial value of σ_3' for each element. It may be seen that σ_3' is reduced by up to 100% over a zone about 30 m long and 6 to 8 m deep located west of the rupture at the crest. Similarly, there is a substantial reduction in σ_3' in a zone at the base and on the footwall just east of the foundation fault rupture.

Because of their cohesive nature, the core materials will support a crack to more than a few metres depth. However the maximum depth of cracking in the core will be limited by the shear strength of the materials, as the shear strength will limit the height of a near-vertical face that will stand without lateral support in the material. Based on the available strength and unit weight data it may be estimated that the maximum depth of cracking is about 10 to 11 m.

Thus, the results of the analyses indicate that deformations of the embankment will likely result in cracking of the core at the crest in an approximately 30 m long zone extending west of the rupture. Little if any cracking of the core is expected east of the rupture. The cracking at the crest is likely to be primarily transverse to the dam axis, although some longitudinal cracking is also expected.

To examine the depth of core cracking at the crest, the calculated values of effective minor principal stress, σ_3', after fault rupture were compared to those before rupture for several profiles through the core in the area of expected cracking. For example, the variation in σ_3' with elevation, before and after rupture, for a profile located on the dam axis 1 m west of the vertical projection of the foundation rupture is shown in Figure 8. Stress changes on that profile are illustrative of changes in the zone of expected cracking along the crest of the dam. The calculated values of σ_3' after rupture are essentially zero to a depth of 5 m (elevation 266). Thus, it may be concluded that cracking is likely to extend to that depth at this location of the crest. Likewise, the zone between 5 and 10 m depth may be thought of as a zone of "incipient" cracking because the calculated values of σ_3' in that zone are low. No cracking of the core is expected below a depth of about 10 m.

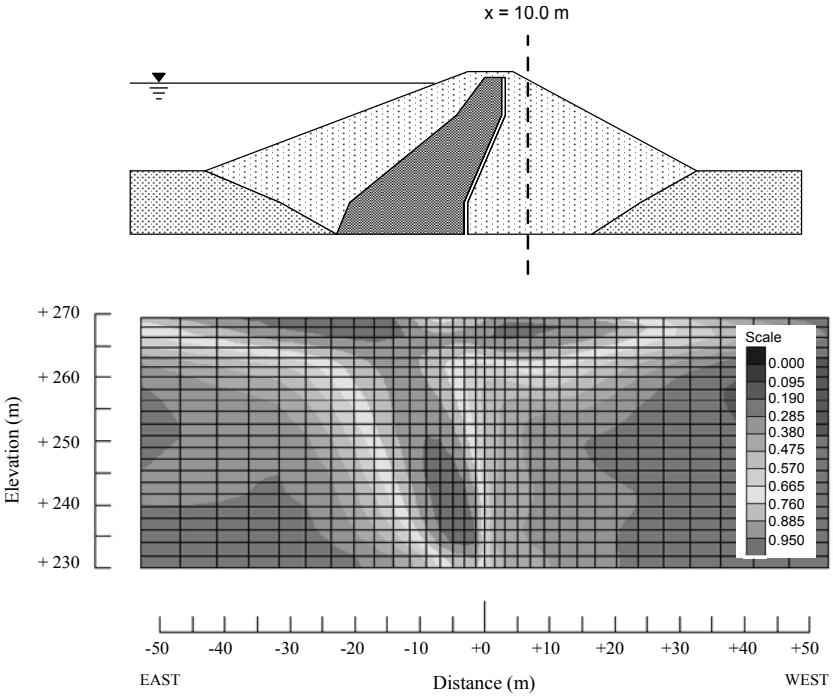

Figure 5. Contours of Stress Level 10 m Downstream of Crest Axis, Calculated Using Hyperbolic Model for 0.5 m Fault Vertical Separation.

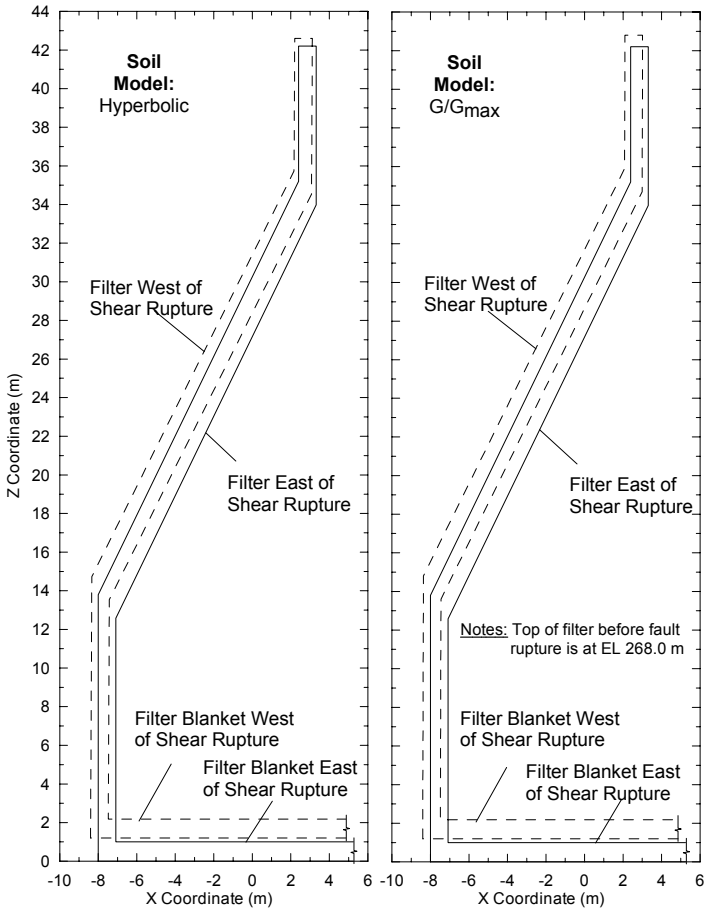

Figure 6. Calculated Shear Offset of Filter.

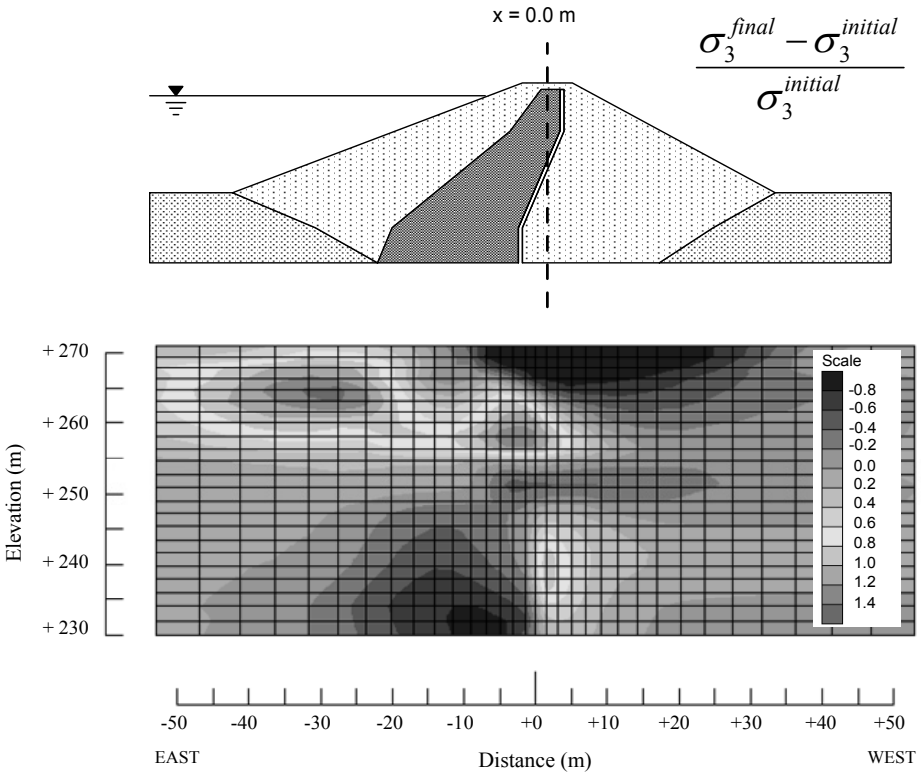

Note: Zero east-west coordinate corresponds to fault location at base of dam.

Figure 7. Change in effective minor principal stress beneath crest axis calculated using hyperbolic model for a fault vertical separation of 1.2 m.

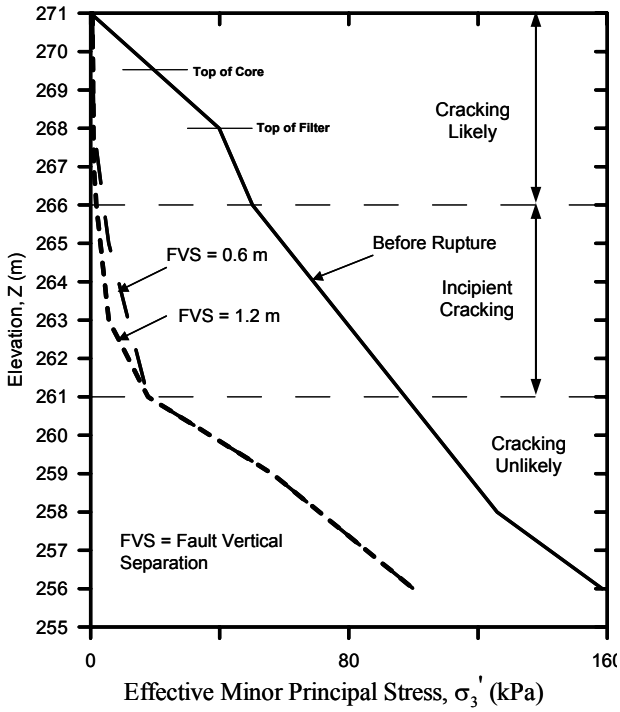

Figure 8. Calculated Depth of Cracking in Dam Core.

ASSESSMENT OF EFFECTS ON EMBANKMENT STABILITY

Cracking caused by fault rupture will be compounded with the effects of earthquake shaking. Tectonic foundation deformations could also increase the severity of cracking, possibly extending the zone of cracking further to the west and increasing the width of cracks. Cracking of the core west of the crest rupture will lead to leakage, because it will extend below the average water level during and after seiche in the reservoir. The leakage will be controlled by the filter, which is expected to remain continuous across the zone of cracking. As the filter remains continuous across the zone of embankment shearing and cracking, it will prevent internal erosion of the embankment materials by the leakage from progressing to a piping failure.

Foundation faulting during the SEE will result in full offset of the filter blanket that extends over the Tertiary sediments at the base of the core trench. The fault zone is a low permeability feature as demonstrated by low piezometric levels and seepage quantities observed downstream of the core. Because the faulted materials have been sheared repeatedly in the past, they are expected to shear again without significant dilation that might lead to a marked increase in permeability. Therefore, it is unlikely that the fault displacements will lead to concentrated leaks or a marked increase in hydraulic gradients through the foundation.

Based on the analyses described above, foundation fault rupture during the SEE is not expected to lead to continued internal erosion of the embankment materials that could progress to a piping failure, or to increased downstream pore water pressures that could result in instability of the embankment dam. However, fault rupture will damage the embankment considerably and may provide a mechanism for continued erosion of the foundation Tertiary sediments into the downstream shoulder as the filter blanket is offset by the fault displacements. In the unlikely event that significant piping occurs, damage sufficient to affect the dam's structural performance is not expected within a period of at least several days after the event.

Evaluations of the dam and its appurtenant works for the effects of strong earthquake shaking and potential overtopping

due to seiche indicate that those effects are also unlikely to lead to failure or instability of the dam [10]. Thus, although the overall post-rupture condition of the embankment would represent a considerable increase in the risk associated with the dam with respect to its pre-earthquake condition, the dam is expected to withstand the SEE without catastrophic release of the reservoir. The dam's post-rupture condition is expected to allow time for emergency response and monitoring of the structure after the event.

CONCLUSIONS

A suitable approach to the seismic evaluation of dams for the effects of earthquake foundation fault displacement has been presented. The approach is based on the key factors to be considered in the evaluation of embankment dams for foundation faulting and addresses the key issues associated with shearing of an embankment dam by fault rupture.

The approach has been illustrated through application to the case history of the seismic safety evaluation of the Aviemore Dam in New Zealand. The dam is a complex structure comprised of a concrete gravity section and an earth embankment. The Waitangi Fault crosses the earth dam foundation near the interface with the concrete dam and extends across the reservoir near its left bank.

The analysis of the dam indicated that foundation fault rupture is not expected to fully offset the dam's chimney filter anywhere along its height. However, full offset is expected to occur across the filter blanket extending downstream over the foundation. Cracking of the impervious core is likely to extend to a depth of about 5 m and "incipient" cracking may occur between 5 and 10 m depth. No cracking of the core is expected below a depth of about 10 m. Cracking of the core will lead to leakage but this will be controlled by the filter, which is expected to remain continuous across the zone of cracking.

Together with other aspects of the seismic evaluation, the analysis of the structural response of the dam to the foundation fault displacements indicates that the dam will withstand the SEE without catastrophic, uncontrolled release of the reservoir.

ACKNOWLEDGEMENTS

The authors thank Meridian Energy for permission to publish this paper. They also wish to acknowledge and thank the large team of professionals from Meridian Energy, URS Corporation, Opus International Consultants, the New Zealand Institute of Geological and Nuclear Sciences, and Meridian's Independent Review Board who contributed to the seismic safety evaluation of Aviemore Dam. The comments by anonymous reviewers of the manuscript helped improve the paper and are kindly appreciated.

REFERENCES

1. Newmark, N., 1965. Effects of earthquakes on dams and embankments, *Geotechnique,* **15**(2): 139-160.
2. Seed, H.B., 1966. A method for earthquake resistant design of earth dams, *Journal of Soil Mechanics and Foundations Division, ASCE*, **92**(SM1): 13-41.
3. Bray, J.D., 1990. The effects of tectonic movements on stresses and deformations in earth embankments, *Ph.D. Thesis*, *University of California, Berkeley*, California, USA.
4. Lazarte, C. A. (1996). "The response of earth structures to surface fault rupture," Ph.D. Thesis, *University of California, Berkeley*, California, USA.
5. Berryman, K., Webb, T., Hill, N., Stirling, M., Rhoades, D., Beavan, J., Darby, D., 2002. Seismic Loads on Dams – Waitaki System – Earthquake Source Characterization, Client Report 2001/129, *Institute of Geological and Nuclear Sciences,* New Zealand.
6. Barrell, D.J., Van Dissen, R.J., Berryman, K.R., Read, S.A., Wood, P.R., Zachariasen, J., Lukovic, B., Nicol, A., Litchfield, N., 2002. Aviemore Power Station – Geological Investigations for Fault Displacement Characterization, Client Report 2001/125, *Institute of Geological and Nuclear Sciences*, New Zealand.
7. Mejia, L., Gillon, M., Walker, J., Newson, T., 2001. Criteria for Developing Seismic Loads for the Safety Evaluation of Dams for Two New Zealand Owners, *Proceedings of NZSOLD/ANCOLD Conference on Dams*, Auckland, New Zealand.
8. Mejia, L., Macfarlane, D., Read, S., Walker, J., 2005. Seismic Criteria for Safety Evaluation of Aviemore Dam, *Proceedings of United States Society on Dams Annual Conference*, Salt Lake City, Utah, USA, Session 6A, 12pp.
9. Walker, J., Gillon, M., and Mejia, L., 2004. Safety Assessment for Active Faulting within the Aviemore Dam Foundation and Reservoir, New Zealand, *Proceedings of ANCOLD 2004 Conference*, Melbourne, Australia.
10. Mejia L., Walker, J., Gillon, M., 2006. Seismic Safety Evaluation of Dam for Foundation Faulting, *Proceedings of δ^{th} National Conference on Earthquake Engineering - 100th Anniversary Earthquake Conference Commemorating the 1906 San Francisco Earthquake*, San Francisco, California, USA, April.
11. Itasca Consulting Group, 2002. FLAC3D, Version 2.10. Fast Lagrangian Analysis of Continua in 3 Dimensions, User's Manual, Minneapolis, Minnesota, USA.
12. Duncan, J. M., Byrne, P., Wong, K. S., and Mabry, P. (1980) "Strength, stress-strain and bulk modulus parameters for finite element analyses of stresses and movements of soil masses." Report No. UCB/GT/80-01, *University of California, Berkeley*, USA.
13. Marachi, N. (1969) "Strength and deformation characteristics of rockfill materials," Ph.D. thesis, *Department of Civil Engineering, University of California, Berkeley*.
14. Seed, H.B. and Idriss, I.M. (1970). "Soil moduli and damping factors for dynamic response analyses," Report EERC 70-10, *Earthquake Engineering Research Centre, University of California, Berkeley*.
15. Vucetic, M. and Dobry, R. (1991). "Effect of soil plasticity on cyclic response," *Journal of Geotechnical Engineering, ASCE*, **117**(1): 89-107.
16. Bray, J. D., Seed, R. B., Seed, H.B. (1994). "Analysis of earthquake fault rupture propagation through cohesive soil," *Journal of Geotechnical Engineering, ASCE,* **120**(3): 562-580.